

Johnson Matthey Highlights

A selection of recent publications by Johnson Matthey R&D staff and collaborators

Flat and Efficient HCNN and CNW Pincer Ruthenium Catalysts for Carbonyl Compound Reduction

S. Giboulot, S. Baldino, M. Ballico, R. Figliolia, A. Pöthig, S. Zhang, D. Zuccaccia and W. Baratta, *Organometallics*, 2019, **38**, (5), 1127

$\text{RuCl}_3 \cdot x\text{H}_2\text{O}$, $[\text{RuCl}_2(\text{CO})_2]_n$, $[\text{RuCl}_2(\text{PPh}_3)_2(\text{dmf})(\text{CO})]$, $[\text{Ru}(\text{OAc})_2(\text{PPh}_3)_2(\text{CO})]$ and *cis*- $[\text{RuCl}(\text{CNW})(\text{PPh}_3)_2]$ precursors were used to synthesise bidentate HCNN *trans*- $[\text{RuX}_2(\text{HCNN})(\text{L})(\text{CO})]$ (X = Cl, OAc) and pincer CNW $[\text{RuCl}(\text{CNW})(\text{L})(\text{CO})]$ (HCNN = Hamtp, Hambq, Hambq^{Ph}; L = CO, PPh₃) carbonyl complexes. In the presence of phosphine (PPh₃ or PCy₃), the monocarbonyl complexes and dicarbonyl derivatives were shown to catalyse the transfer hydrogenation (TH) of acetophenone in 2-propanol at reflux and the TH of carbonyl compounds (including bulky ketones and β-unsaturated aldehydes).

Technical Considerations for Scale-Up of Imine-Reductase-Catalyzed Reductive Amination: A Case Study

A. Bornadel, S. Bisagni, A. Pushpanath, S. L. Montgomery, N. J. Turner and B. Dominguez, *Org. Process Res. Dev.*, 2019, **23**, (6), 1262

Imine reductases (IREDs) can be used as biocatalysts for the synthesis of various cyclic and acyclic amines. The development and scale-up of such reactions was considered based on the reductive amination of cyclohexanone with cyclopropylamine. Various reaction parameters were studied using a design of experiments approach, which identified enzyme stability as the limiting factor. Kinetic studies demonstrated that IRED-33 was the most stable enzyme for the reaction. In an 8 h period, and under optimal reaction conditions, 100% conversion to the desired amine was achieved from the reaction of cyclohexanone and cyclopropylamine at 750 mM concentration.

Accurate 3D Characterization of Catalytic Bodies Surface by Scanning Electron Microscopy

L. C. Gontard, M. Á. Cauqui, M. P. Yeste, D. Ozkaya and J. J. Calvino, *ChemCatChem*, 2019, **11**, (14), 3171

Industrial catalysis often uses catalytic bodies of millimetric dimensions. The chemical and spatial relations of the exposed surface of the catalytic device are affected by the raw nanocatalyst engineering process. It is therefore vital to understand the heterogeneities of catalytic device surfaces to improve their synthesis. Three-dimensional and high resolution physico-chemical characterisation was performed on the surface of commercial water gas shift catalyst bodies using a combination of photogrammetry, scanning electron microscopy and X-ray spectroscopy. The measurements observed from these methods were shown to be reliable, accurate and precise.

Slurry Loop Tubular Membrane Reactor for the Catalysed Aerobic Oxidation of Benzyl Alcohol

B. Venezia, M. Douthwaite, G. Wu, M. Sankar, P. Ellis, G. J. Hutchings and A. Gavriilidis, *Chem. Eng. J.*, 2019, **378**, 122250

A novel slurry loop reactor was designed and implemented for the aerobic oxidation of benzyl alcohol using a 1 wt% Au-Pd/TiO₂ powdered catalyst. Safe and controlled oxygen delivery was achieved with the incorporation of a tubular membrane. In comparison to a conventional autoclave reactor, the slurry loop reactor demonstrated similar oxidation turnover frequency and benzaldehyde selectivity (20,000–25,000 h⁻¹ and 70%, respectively). To allow for continuous operation, a crossflow filter was inserted inside the loop to prevent the catalyst from exiting the reactor. Undertaking continuous reactions showed that increasing the external oxygen pressure or decreasing the reaction temperature increased

benzaldehyde selectivity. Applications that are limited by gaseous reactant availability, use a powder catalyst and require safe operation could benefit from the slurry loop reactor.

Modelling Reaction and Diffusion in a Wax-Filled Hollow Cylindrical Pellet of Fischer Tropsch Catalyst

R. Hubble, A. P. E. York and J. S. Dennis, *Chem. Eng. Sci.*, 2019, **207**, 958

A pseudo-isothermal, steady-state, two-dimensional (2D) model was investigated for the Fischer-Tropsch (FT) reaction for solid and hollow cylindrical cobalt-based catalyst pellets. The Co-based catalyst was considered at conditions where liquid hydrocarbons accumulate in the pores. Comparisons were made with sphere and slab models. With regard to effectiveness factor, slab and sphere values were exceeded between the Thiele moduli range of 0.75–1.15. However, with the FT chain growth parameter, the values were lower than slab and sphere geometry. Therefore, hollow cylinders under these conditions demonstrated the greatest selectivity towards methane.

Opportunities and Challenges for Catalysis in Carbon Dioxide Utilization

M. D. Burkart, N. Hazari, C. L. Tway and E. L. Zeitler, *ACS Catal.*, 2019, **9**, (9), 7937

In carbon dioxide (CO₂) utilisation processes, CO₂ is either used directly or converted into more valuable products. Such processes will be vital for reducing CO₂ emissions in our atmosphere. The successful conversion of CO₂ to value-added products will be heavily reliant on catalysis. This paper provides a review of the biological and chemical systems for CO₂ utilisation, along with the specific and more general challenges that will be presented. Comparisons are drawn between various methods of CO₂ conversion, for instance homogeneous vs. heterogeneous catalysis and photosynthetic vs. nonphotosynthetic biological conversion. Issues with CO₂ conversion are also identified, which will need to be addressed by the technology.

Toward Stable Electrode/Electrolyte Interface of P2-Layered Oxide for Rechargeable Na-Ion Batteries

M. Zarrabeitia, L. G. Chagas, M. Kuenzel, E. Gonzalo, T. Rojo, S. Passerini and M. Á. Muñoz-Márquez, *ACS Appl. Mater. Interfaces*, 2019, **11**, (32), 28885

P2-Na_{2/3}Mn_{0.8}Fe_{0.1}Ti_{0.1}O₂ layered oxide has potential as a cathode material for rechargeable Na-ion batteries (NIBs). An optimised ionic liquid (IL)-based electrolyte was used to evaluate the electrochemical properties of P2-Na_{2/3}Mn_{0.8}Fe_{0.1}Ti_{0.1}O₂. In comparison to a carbonate-based electrolyte, the IL-based electrolyte demonstrated better electrochemical performance at room temperature. Cycling stability was also particularly strong, with a 97% capacity

retention after 100 deep cycles. Scanning electron microscopy and X-ray photoelectron spectroscopy were employed to study the electrode/electrolyte interface in both systems. The IL-based system had a thinner, more stable and homogenous interface layer. Therefore, such systems could lead to longer-lasting and safer NIBs.

Electronic and Geometric Structures of Rechargeable Lithium Manganese Sulfate Li₂Mn(SO₄)₂ Cathode

D. Gupta, A. Muthiah, M. P. Do, G. Sankar, T. I. Hyde, M. P. Copley, T. Baikie, Y. Du, S. Xi, M. Srinivasan and Z. Dong, *ACS Omega*, 2019, **4**, (7), 11338

The synthesis and characterisation of Li₂Mn(SO₄)₂ (LMS) (**Figure 1**), a potential energy storage material, is described over one electrochemical cycle. LMS was synthesised by ball milling MnSO₄·H₂O and Li₂SO₄·H₂O. A combination of *ex situ* X-ray diffraction, X-ray photoelectron spectroscopy and X-ray absorption spectroscopy were used to characterise LMS. X-ray photoelectron spectroscopy analysis demonstrated changes in the oxidation state of Mn, whereas X-ray absorption spectroscopy analysis suggested minimal changes to the oxidation state of Mn and S ions during charge-discharge cycles. Dominance of electrochemical reactions at the surface of the LMS particles, rather than in the bulk, could explain the difference in the results during cycling.

Extracting Structural Information of Au Colloids at Ultra-Dilute Concentrations: Identification of Growth During Nanoparticle Immobilization

G. F. Tierney, D. Decarolis, N. Abdullah, S. M. Rogers, S. Hayama, M. Briceno de Gutierrez, A. Villa, C. R. A. Catlow, P. Collier, N. Dimitratos and P. P. Wells, *Nanoscale Adv.*, 2019, **1**, (7), 2546

Using sol-immobilisation to achieve supported metal nanoparticles (NPs) ensures a high degree of control of the metal particle size and yields a narrow particle size distribution. In this study, state of the art beamlines and X-ray absorption fine structure techniques were used to provide structural

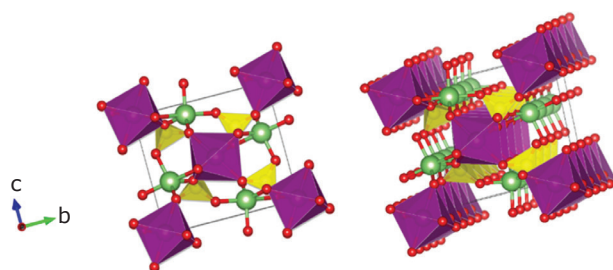


Fig. 1. Reprinted with permission from D. Gupta *et al.*, *ACS Omega*, 2019, **4**, (7), 11338. Copyright (2019) American Chemical Society. Further permissions related to this material should be directed to the ACS

information on nano-sized colloidal Au solutions at μM concentration. By adjusting the temperature of reduction, it was possible to accurately tune the size of Au colloids. It was also demonstrated that Au concentration had little effect on the size of colloidal Au NPs in solution. A significant growth in Au particle size was attributed to the immobilisation step. By understanding the primary steps in sol-immobilisation, the optimisation of materials for catalytic application can be improved.

Ultra-Smooth and Space-Filling Mineral Films Generated *via* Particle Accretion Processes

J. Harris, I. P. Mey, C. F. Böhm, T. T. H. Trinh, S. Leupold, C. Prinz, P. Tripal, R. Palmisano and S. E. Wolf, *Nanoscale Horiz.*, 2019, **4**, (6), 1388

Nonclassical crystallisation is driven by nanoparticle self-organisation. Therefore, it tends to yield materials with pronounced porosity and roughness. In this study, a bio-inspired nonclassical mineralisation approach was taken, *via* magnesium-doped polymer-induced liquid precursors, to generate ultra-smooth and dense calcium carbonate films. The films featured a roughness of 0.285 nm, which is uncharacteristically low for minerals generated *via* nonclassical pathways. The research provides an insight into the role of magnesium in biomineralisation of calcareous species. It also describes a concept for lifting key limitations of nonclassical mineralisation pathways.

Improvements to the Production of ZIF-94; A Case Study in MOF Scale-Up

T. Johnson, M. M. Łozińska, A. F. Orsi, P. A. Wright, S. Hindocha and S. Poulston, *Green Chem.*, 2019, **21**, (20), 5665

Metal organic frameworks (MOFs) have shown remarkable promise at the laboratory scale. Large-scale production is essential for their successful commercialisation. This study demonstrates improvements in the production of ZIF-94 from ~ 1 g laboratory preparation to a scalable procedure. Conditions for the ZIF-94 synthesis included atmospheric pressure and room temperature. Unlike current synthesis routes, dimethylformamide was not used as a solvent. The weight percent of solids from this method was higher than previously reported synthetic routes, at 18 wt%. A large scale (60 g) production of the framework was produced to highlight the robustness of the derived methodology. Overall, ZIF-94 production demonstrated improved concentration, improved CO_2 uptake, maintained nano-morphology and reduced costs.

Impact of Carbon Support Corrosion on Performance Losses in Polymer Electrolyte Membrane Fuel Cells

F. Hegge, J. Sharman, R. Moroni, S. Thiele, R. Zengerle, M. Breitwieser and S. Vierrath, *J. Electrochem. Soc.*, 2019, **166**, (13), F956

Membrane electrode assemblies (MEAs) were cycled between 1–1.5 V in order to study the effect of degradation on oxygen transport. Focused ion beam-scanning electron microscope (FIB-SEM) tomography was used at various ageing states to analyse electrode structure. Results demonstrated that electrode structure (porosity, thickness and diffusivity) changed over 1000 cycles. The pressure independent resistance increased from 24 sm^{-1} to 41 sm^{-1} . 50% of this increase was attributed to an increased local mass transport resistance and 44% from a change in the wetting behaviour. 6% of the increase remains unexplained.